Journal of Advances in Nanomaterials, Vol. 4, No. 2, June 2019
https://dx.doi.org/10.22606/jan.2019.42003

Effect of Interface Energy on Scattering of Plane Compressional Wave by a Cylinder with an Eccentric Inclusion

D. X. Lei, C. X. Zhang, Z. Y. Ou*

School of Science, Lanzhou University of Technology, Gansu, Lanzhou, 730050 China
Email: zhiyingou@163.com

Abstract. The wave function expansion and addition theorem are used in the solution of dynamic stress concentration factor around a cylinder with an eccentric inclusion at nano-scale. Stresses satisfy the Young-Laplace equations and displacements are continuous on the surface. For incident waves with different frequencies, surface effects, softer/hard inclusion and core eccentricity on the dynamic stress concentration factor are discussed. The incident wave frequency, surface effects, softer/hard inclusion and core eccentricity have significant effects on the dynamic on the dynamic stress concentration factor as the radius of the inclusion shrinks to the nanoscale.

Keywords: Scattering, plane compressional wave, eccentric inclusion, dynamic stress concentration factor

1 Introduction

The problem of normally incident plane wave scattered by an eccentric metallic cylinder coated with a dielectric cylindrical layer was solved, and several authors have presented studies on the scattered electromagnetic fields from eccentric cylindrical structures. For example, Hasheminejad and Kazemirad [1-3] investigated exact solution for a harmonic plane acoustic wave with a circular cylinder which is eccentrically coated by another material. Mushref [4] found a solution for the problem of two infinite axial slots in a thin circular cylinder enclosed by an eccentric dielectric material. Simao and Guimaraes [5] analyzed the resonant scattering of light by a dielectric cylinder with an eccentric cylindrical metallic inclusion. Roumeliotis and Fikioris [6] analyzed the cutoff wavenumbers and the field of surface wave modes of a circular cylindrical conductor eccentrically coated by a dielectric. Pattanayak [7] studied the effect of axially uniform eccentricity on the modal structures and velocitie in circular tubes or pipes. Mushref [8] realized closed series solution to scattering by an eccentric coated cylinder in matrix form. Yousif and Elsherbeni [9] analyzed the scattering of electromagnetic plane waves from a multi-eccentric cylinder at oblique incidence. Weber and Zastrau [10] derived the scattering behaviour of a single multi-layered inclusion in a homogeneousisotropic matrix under the influence of non-plane elastic SH waves. Huang *et al.* [11] studied the scattering of an elastic wave obliquely incident on a multilayered cylinder in a solid. Qin *et al.* [12] analyzed three kinds of resonant modes of a single layered circular elastic cylinder embedded in the elastic medium. Hasheminejad and Rajabi [13] employed exact treatment based on the inherent background coefficients that describe the background amplitudes in the scattered field. Shindo and Niwa [14] dealed with the scattering of antiplane shear waves in a metal matrix composite reinforced by fibers with interracial layers. Li *et al.* [15] studied the scattering and dynamic stress concentration in fiber-reinforced composite with interfaces. Nersisyan and Matevosyan [16] considered the scattering and transformation of the waves propagating in magnetized plasma on a heavy stationary charged particle located at a plane plasma-vacuum boundary. Godoy and Villa [17] derived such exact wave function for a beam of Dirac and Klein-Gordon particles. Yahya *et al.* [18] discussed the effect of initial stress on the radial vibrations of elastic hollow cylinder with ro-tation. Volobuev and Petro [19] showed that the start of electrons from atom at a photoeffect is almost spherical symmetric. El-Shorbagy *et al.* [20] discussed the stabilization effect of a strong HF electric field on beam-plasma instability in a cylindrical warm plasma waveguide.

However, in the aforementioned studies, the effect of the interface stress was not taken into account. Wang [21] considered the diffraction of P-wave by a nanosized circular hole. Wang [22] investigated the multiple diffractions of plane harmonic compressional waves by two nanosized circular cylindrical holes embedded in an elastic solid. Ru *et al.* [23] described the diffraction of elastic waves and the stress

Copyright © 2019 Isaac Scientific Publishing

concentration near a cylindrical nano-inclusion with surface effect. Ou [24] studied the scattering of plane compressional and shear waves by a single nano-sized coated fiber embedded in an elastic matrix using the method of eigenfunction expansion. Ou [25] investigated the multiple scattering of plane compressional waves by two cylindrical fibers with interface effects.

In this study, we examined the scattering of an elastic wave by a cylinder with an eccentric inclusion. The interface stresses at the inner and outer interfaces of the annular-coated layer are considered. Using the method of wave function expansion and addition theorem, the dynamic elastic fields were derived and numerically calculated. The dynamic stress concentration factors (DSCF) along the interface were obtained. The results show that the influence of the interface stresses on the DSCF becomes significant when the radius of the inclusion is reduced to the nanometer scale.

2 Model Analysis and Formulation

Based on the surface elasticity, we considered the scattering of an elastic wave by a by a cylinder with an eccentric inclusion, as shown in Fig. 1. Two circles with O_1, O_2 as the center and b, a as the inner and outer radius, respectively, the distance between the two centers is d. The elastic constants and the densities of the matrix, coating and inclusion are $\lambda^{(j)}$, $\mu^{(j)}$ and $\rho^{(j)}$ (j=0, 1, 2) respectively, where the superscripts 0, 1, and 2 indicate the quantities associated with the matrix, coating, and core, respectively.

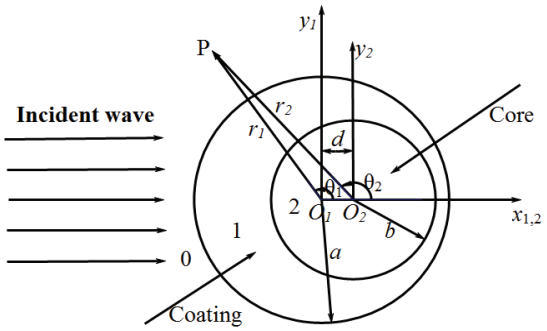

Figure 1. Cross section of scattering of incident wave by a cylindrical with an eccentric inclusion.

In the cylindrical coordinate system (r_1,θ_1), the displacement potential of the incident wave can be written as

$$\varphi^{\text{inc}}(r_1,\theta_1) = \varphi_0 \sum_{n=-\infty}^{\infty} \mathrm{i}^n J_n(\alpha_0 r_1)\mathrm{e}^{\mathrm{i}n\theta_1}\mathrm{e}^{-\mathrm{i}\omega t}, \tag{1}$$

where φ_0 is the amplitude of the incident wave, the superscript inc represents incident wave, $\alpha_0 = \omega/c_p^{(0)}$ is the wave number of the matrix, and $c_p^{(0)} = \sqrt{\left(\lambda^{(0)} + 2\mu^{(0)}\right)/\rho^{(0)}}$ is the wave velocity, i is the unit of imaginary number, t is time, $J_n(x)$ is the nth order Bessel function of the first kind.

When it impinges on the coated, the P wave and SV wave are scattered back from the interface (r_1=a), and the corresponding displacement potentials of the scattered wave are given by

$$\varphi^{\text{sca}}\left(r_1,\theta_1\right) = \varphi_0 \sum_{n=-\infty}^{\infty} A_n H_n^{(1)}\left(\alpha_0 r_1\right)\mathrm{e}^{\mathrm{i}n\theta_1}\mathrm{e}^{-\mathrm{i}\omega t}, \tag{2a}$$

$$\psi^{\text{sca}}(r_1,\theta_1) = \varphi_0 \sum_{n=-\infty}^{\infty} B_n H_n^{(1)}(\beta_0 r_1)\mathrm{e}^{\mathrm{i}n\theta_1}\mathrm{e}^{-\mathrm{i}\omega t}, \tag{2b}$$

where A_n and B_n are unknown coefficients, the superscript sca represents scattering wave, $H_n^{(1)}\left(x\right)$ is the nth order Hankel function of the first kind, $\beta_0 = \omega/c_s^{(0)}$ is the SV-wave number of the matrix, and $c_s^{(0)} = \sqrt{\mu^{(0)}/\rho^{(0)}}$ is the shear wave velocity.

So the total waves in the matrix are determined by the superposition of the incident waves and scattered waves.

Copyright © 2019 Isaac Scientific Publishing

$$\varphi^{(0)}\left(r_1,\theta_1\right)=\varphi^{\mathrm{inc}}\left(r_1,\theta_1\right)+\varphi^{\mathrm{sca}}\left(r_1,\theta_1\right), \tag{3a}$$

$$\psi^{(0)}\left(r_1,\theta_1\right)=\psi^{\mathrm{sca}}\left(r_1,\theta_1\right). \tag{3b}$$

The standing compressional and shear waves reverberating inside the dissipative interphase are described as

$$\varphi^{(1)}=\varphi_0\sum_{n=-\infty}^{\infty}\left[C_nJ_n(\alpha_1r_1)\mathrm{e}^{\mathrm{i}n\theta_1}+D_nH_n^{(1)}(\alpha_1r_2)\mathrm{e}^{\mathrm{i}n\theta_2}\right]\mathrm{e}^{-\mathrm{i}\omega t}, \tag{4a}$$

$$\psi^{(1)}=\varphi_0\sum_{n=-\infty}^{\infty}\left[E_nJ_n\left(\beta_1r_1\right)\mathrm{e}^{\mathrm{i}n\theta_1}+F_nH_n^{(1)}\left(\beta_1r_2\right)\mathrm{e}^{\mathrm{i}n\theta_2}\right]e^{-\mathrm{i}\omega t}. \tag{4b}$$

where C_n, D_n, E_n, and F_n are unknown coefficients in coating; and $\alpha_1=\omega/c_p^{(1)}$, $\beta_1=\omega/c_s^{(1)}$ where $c_p^{(1)}=\sqrt{\left(\lambda^{(1)}+2\mu^{(1)}\right)/\rho^{(1)}}$ and $c_s^{(1)}=\sqrt{\mu^{(1)}/\rho^{(1)}}$.

The refracted waves in core can be transformed as

$$\varphi^{(2)}(r_2,\theta_2)=\varphi_0\sum_{n=-\infty}^{\infty}G_nJ_n(\alpha_2r_2)\mathrm{e}^{\mathrm{i}n\theta_2}\mathrm{e}^{-\mathrm{i}\omega t}, \tag{5a}$$

$$\psi^{(2)}(r_2,\theta_2)=\varphi_0\sum_{n=-\infty}^{\infty}K_nJ_n(\beta_2r_2)\mathrm{e}^{\mathrm{i}n\theta_2}\mathrm{e}^{-\mathrm{i}\omega t}. \tag{5b}$$

By Graf's addition theorem for Bessel functions, the transformation between two local coordinate systems can be expressed by

$$H_n(kr_2)\mathrm{e}^{\mathrm{i}n\theta_2}=\sum_{m=-\infty}^{\infty}J_{m-n}(kd)H_m(kr_1)\mathrm{e}^{\mathrm{i}m\theta_1}, \tag{6a}$$

$$J_n\left(kr_1\right)\mathrm{e}^{\mathrm{i}n\theta_1}=\sum_{m=-\infty}^{\infty}J_{n-m}\left(kd\right)J_m\left(kr_2\right)\mathrm{e}^{\mathrm{i}m\theta_2}, \tag{6b}$$

Therefore, in the coordinate system (r_1,θ_1), Eq. (4) can be deduced from Eq. (6) as

$$\varphi^{(1)}\left(r_1,\theta_1\right)=\varphi_0\sum_{n=-\infty}^{\infty}\left[C_nJ_n(\alpha_1r_1)\mathrm{e}^{\mathrm{i}n\theta_1}+\sum_{m=-\infty}^{\infty}D_nJ_{m-n}(\alpha_1d)H_m^{(1)}(\alpha_1r_1)\mathrm{e}^{\mathrm{i}m\theta_1}\right]\mathrm{e}^{-\mathrm{i}\omega t}, \tag{7a}$$

$$\psi^{(1)}\left(r_1,\theta_1\right)=\varphi_0\sum_{n=-\infty}^{\infty}\left[E_nJ_n(\beta_1r_1)\mathrm{e}^{\mathrm{i}n\theta_1}+\sum_{m=-\infty}^{\infty}F_nJ_{m-n}(\beta_1d)H_m^{(1)}(\beta_1r_1)\mathrm{e}^{\mathrm{i}m\theta_1}\right]\mathrm{e}^{-\mathrm{i}\omega t}, \tag{7b}$$

In the coordinate system (r_2,θ_2), Eq. (4) can be written as

$$\varphi^{(1)}(r_2,\theta_2)=\varphi_0\sum_{n=-\infty}^{\infty}\left[\sum_{m=-\infty}^{\infty}C_nJ_{n-m}(\alpha_1d)J_m(\alpha_1r_2)\mathrm{e}^{\mathrm{i}m\theta_2}+D_nH_n^{(1)}(\alpha_1r_2)\mathrm{e}^{\mathrm{i}n\theta_2}\right]\mathrm{e}^{-\mathrm{i}\omega t}, \tag{8a}$$

$$\psi^{(1)}(r_2,\theta_2)=\varphi_0\sum_{n=-\infty}^{\infty}\left[\sum_{m=-\infty}^{\infty}E_nJ_{n-m}(\beta_1d)J_m(\beta_1r_2)\mathrm{e}^{\mathrm{i}m\theta_2}+F_nH_n^{(1)}(\beta_1r_2)\mathrm{e}^{\mathrm{i}n\theta_2}\right]\mathrm{e}^{-\mathrm{i}\omega t}, \tag{8b}$$

Furthermore, the relevant displacement components in polar coordinates in terms of compressional and shear wave potentials are

$$u_r=\frac{\partial\varphi}{\partial r}+\frac{1}{r}\frac{\partial\psi}{\partial\theta}, \tag{9a}$$

$$u_\theta=\frac{1}{r}\frac{\partial\varphi}{\partial\theta}-\frac{\partial\psi}{\partial r}, \tag{9b}$$

and the corresponding stresses in compound cylinder read

$$\sigma_{rr}=\lambda\left(\frac{\partial^2\varphi}{\partial r^2}+\frac{1}{r}\frac{\partial\varphi}{\partial r}+\frac{1}{r^2}\frac{\partial^2\varphi}{\partial\theta^2}\right)+2\mu\left(\frac{\partial^2\varphi}{\partial r^2}-\frac{1}{r^2}\frac{\partial\psi}{\partial\theta}+\frac{1}{r}\frac{\partial^2\psi}{\partial r\partial\theta}\right), \tag{10a}$$

$$\sigma_{\theta\theta}=\lambda\left(\frac{\partial^2\varphi}{\partial r^2}+\frac{1}{r}\frac{\partial\varphi}{\partial r}+\frac{1}{r^2}\frac{\partial^2\varphi}{\partial\theta^2}\right)+2\mu\left(\frac{1}{r^2}\frac{\partial^2\varphi}{\partial\theta^2}+\frac{1}{r}\frac{\partial\varphi}{\partial r}-\frac{1}{r}\frac{\partial^2\psi}{\partial r\partial\theta}+\frac{1}{r^2}\frac{\partial\psi}{\partial\theta}\right), \tag{10b}$$

 Copyright © 2019 Isaac Scientific Publishing

$$\sigma_{r\theta}=\frac{\mu}{r}\left(2\frac{\partial^2\varphi}{\partial r\partial\theta}-\frac{2}{r}\frac{\partial\varphi}{\partial\theta}+\frac{1}{r}\frac{\partial^2\psi}{\partial\theta^2}-r\frac{\partial^2\psi}{\partial r^2}+\frac{\partial\psi}{\partial r}\right). \tag{10c}$$

We omit the time factor of $e^{-i\omega t}$. Substituting Eqs. (3), (5), (7) and (8) into Eqs. (9) and (10), we can obtain the displacements of the matrix, coating and core.

$$u_{r_2}^{(1)}=\frac{\varphi_0}{r_2}\sum_{n=-\infty}^{\infty}\left(M_{71}^{(3)}(\alpha_1 r_2)D_n+iM_{72}^{(3)}(\beta_1 r_2)F_n\right)e^{in\theta_2}$$

$$+\frac{\varphi_0}{r_2}\sum_{m=-\infty}^{\infty}\sum_{n=-\infty}^{\infty}\left(J_{n-m}(\alpha_1 d)M_{71}^{(1)}(\alpha_1 r_2)C_n+J_{n-m}(\beta_1 d)iM_{72}^{(1)}(\beta_1 r_2)E_n\right)e^{im\theta_2}, \tag{11a}$$

$$u_{r_2}^{(2)}=\frac{\varphi_0}{r_2}\sum_{n=-\infty}^{\infty}\left(M_{71}^{(1)}(\alpha_2 r_2)G_n+iM_{72}^{(1)}(\beta_2 r_2)K_n\right)e^{in\theta_2} \tag{11b}$$

$$u_{\theta_2}^{(1)}=\frac{\varphi_0}{r_2}\sum_{n=-\infty}^{\infty}\left(iM_{81}^{(3)}(\alpha_1 r_2)D_n+M_{82}^{(3)}(\beta_1 r_2)F_n\right)e^{in\theta_2}$$

$$+\frac{\varphi_0}{r_2}\sum_{m=-\infty}^{\infty}\sum_{n=-\infty}^{\infty}\left(J_{n-m}(\alpha_1 d)iM_{81}^{(1)}(\alpha_1 r_2)C_n+J_{n-m}(\beta_1 d)M_{82}^{(1)}(\beta_1 r_2)E_n\right)e^{im\theta_2}, \tag{11c}$$

$$u_{\theta_2}^{(2)}=\frac{\varphi_0}{r_2}\sum_{n=-\infty}^{\infty}\left(iM_{81}^{(1)}(\alpha_2 r_2)G_n+M_{82}^{(1)}(\beta_2 r_2)K_n\right)e^{in\theta_2}, \tag{11d}$$

$$u_{r_1}^{(0)}=\frac{\varphi_0}{r_1}\sum_{n=-\infty}^{\infty}\left(M_{71}^{(1)}(\alpha_0 r_1)i^n+M_{71}^{(3)}(\alpha_0 r_1)A_n+iM_{72}^{(3)}(\beta_0 r_1)B_n\right)e^{in\theta_1}, \tag{12a}$$

$$u_{\theta_1}^{(0)}=\frac{\varphi_0}{r_1}\sum_{n=-\infty}^{\infty}\left(M_{81}^{(1)}(\alpha_0 r_1)i^{n+1}+iM_{81}^{(3)}(\alpha_0 r_1)A_n+M_{82}^{(3)}(\beta_0 r_1)B_n\right)e^{in\theta_1}, \tag{12b}$$

$$u_{r_1}^{(1)}=\frac{\varphi_0}{r_1}\sum_{n=-\infty}^{\infty}\left(M_{71}^{(1)}(\alpha_1 r_1)C_n+iM_{72}^{(1)}(\beta_1 r_1)E_n\right)e^{in\theta_1}$$

$$+\frac{\varphi_0}{r_1}\sum_{m=-\infty}^{\infty}\sum_{n=-\infty}^{\infty}\left(J_{m-n}(\alpha_1 d)M_{71}^{(3)}(\alpha_1 r_1)D_n+J_{m-n}(\beta_1 d)iM_{72}^{(3)}(\beta_1 r_1)F_n\right)e^{im\theta_1}, \tag{12c}$$

$$u_{\theta_1}^{(1)}=\frac{\varphi_0}{r_1}\sum_{n=-\infty}^{\infty}\left(iM_{81}^{(1)}(\alpha_1 r_1)C_n+M_{82}^{(1)}(\beta_1 r_1)E_n\right)e^{in\theta_1}$$

$$+\frac{\varphi_0}{r_1}\sum_{m=-\infty}^{\infty}\sum_{n=-\infty}^{\infty}\left(J_{m-n}(\alpha_1 d)iM_{81}^{(3)}(\alpha_1 r_1)D_n+J_{m-n}(\beta_1 d)M_{82}^{(3)}(\beta_1 r_1)F_n\right)e^{im\theta_1}, \tag{12d}$$

The corresponding stresses are

$$\sigma_{r_2r_2}^{(2)}=\frac{2\mu^{(2)}\varphi_0}{r_2^2}\sum_{n=-\infty}^{\infty}\left(E_{11}^{(1)}(\alpha_2 r_2)G_n+iE_{12}^{(1)}(\beta_2 r_2)K_n\right)e^{in\theta_2}, \tag{13a}$$

$$\sigma_{r_2r_2}^{(1)}=\frac{2\mu^{(1)}\varphi_0}{r_2^2}\sum_{n=-\infty}^{\infty}\left(E_{11}^{(3)}(\alpha_1 r_2)D_n+iE_{12}^{(3)}(\beta_1 r_2)F_n\right)e^{in\theta_2}$$

$$+\frac{2\mu^{(1)}\varphi_0}{r_2^2}\sum_{m=-\infty}^{\infty}\sum_{n=-\infty}^{\infty}\left(J_{n-m}(\alpha_1 d)E_{11}^{(1)}(\alpha_1 r_2)C_n+J_{n-m}(\beta_1 d)iE_{12}^{(1)}(\beta_1 r_2)E_n\right)e^{im\theta_2}, \tag{13b}$$

$$\sigma_{\theta_2\theta_2}^{(2)}=\frac{2\mu^{(2)}\varphi_0}{r_2^2}\sum_{n=-\infty}^{\infty}\left(E_{21}^{(1)}(\alpha_2 r_2)G_n+iE_{21}^{(3)}(\beta_2 r_2)K_n\right)e^{in\theta_2}, \tag{13c}$$

$$\sigma_{r_2\theta_2}^{(1)}=\frac{2\mu^{(1)}\varphi_0}{r_2^2}\sum_{n=-\infty}^{\infty}\left(iE_{41}^{(3)}(\alpha_1 r_2)D_n+E_{42}^{(3)}(\beta_1 r_2)F_n\right)e^{in\theta_2}$$

Copyright © 2019 Isaac Scientific Publishing

$$+\frac{2\mu^{(1)}\varphi_0}{r_2^2}\sum_{m=-\infty}^{\infty}\sum_{n=-\infty}^{\infty}\left(J_{n-m}\left(\alpha_1 d\right)\mathrm{i}E_{41}^{(1)}\left(\alpha_1 r_2\right)C_n+J_{n-m}\left(\beta_1 d\right)E_{42}^{(1)}\left(\beta_1 r_2\right)E_n\right)\mathrm{e}^{\mathrm{i}m\theta_2}, \tag{14a}$$

$$\sigma_{r_2\theta_2}^{(2)}=\frac{2\mu^{(2)}\varphi_0}{r_2^2}\sum_{n=-\infty}^{\infty}\left(\mathrm{i}E_{11}^{(1)}\left(\alpha_2 r_2\right)G_n+E_{42}^{(1)}\left(\beta_2 r_2\right)K_n\right)\mathrm{e}^{\mathrm{i}n\theta_2}, \tag{14b}$$

$$\sigma_{r_1r_1}^{(1)}=\frac{2\mu^{(1)}\varphi_0}{r_1^2}\sum_{n=-\infty}^{\infty}\left(E_{11}^{(1)}(\alpha_1 r_1)C_n+\mathrm{i}E_{12}^{(1)}(\beta_1 r_1)E_n\right)\mathrm{e}^{\mathrm{i}n\theta_1}$$

$$+\frac{2\mu^{(1)}\varphi_0}{r_1^2}\sum_{m=-\infty}^{\infty}\sum_{n=-\infty}^{\infty}\left(J_{m-n}\left(\alpha_1 d\right)E_{11}^{(3)}\left(\alpha_1 r_1\right)D_n+\mathrm{i}J_{m-n}\left(\beta_1 d\right)E_{12}^{(3)}\left(\beta_1 r_1\right)F_n\right)\mathrm{e}^{\mathrm{i}m\theta_1}, \tag{15a}$$

$$\sigma_{r_1r_1}^{(0)}=\frac{2\mu^{(0)}\varphi_0}{r_1^2}\sum_{n=-\infty}^{\infty}\left(E_{11}^{(1)}\left(\alpha_0 r_1\right)\mathrm{i}^n+E_{11}^{(3)}\left(\alpha_0 r_1\right)A_n+\mathrm{i}E_{12}^{(3)}\left(\beta_0 r_1\right)B_n\right)\mathrm{e}^{\mathrm{i}n\theta_1}, \tag{15b}$$

$$\sigma_{\theta_1\theta_1}^{(0)}=\frac{2\mu^{(0)}\varphi_0}{r_1^2}\sum_{n=-\infty}^{\infty}\left(E_{21}^{(1)}(\alpha_0 r_1)\mathrm{i}^n+E_{21}^{(3)}(\alpha_0 r_1)A_n+\mathrm{i}E_{22}^{(3)}(\beta_0 r_1)B_n\right)\mathrm{e}^{\mathrm{i}n\theta_1}, \tag{15c}$$

$$\sigma_{r_1\theta_1}^{(0)}=\frac{2\mu^{(0)}\varphi_0}{r_1^2}\sum_{n=-\infty}^{\infty}\left(E_{41}^{(1)}\left(\alpha_0 r_1\right)\mathrm{i}^{n+1}+\mathrm{i}E_{41}^{(3)}(\alpha_0 r_1)A_n+E_{42}^{(3)}(\beta_0 r_1)B_n\right)\mathrm{e}^{\mathrm{i}n\theta_1}, \tag{16a}$$

$$\sigma_{r_1\theta_1}^{(1)}=\frac{2\mu^{(1)}\varphi_0}{r_1^2}\sum_{n=-\infty}^{\infty}\left(\mathrm{i}E_{41}^{(1)}(\alpha_1 r_1)C_n+E_{42}^{(1)}(\beta_1 r_1)E_n\right)\mathrm{e}^{\mathrm{i}n\theta_1}$$

$$+\frac{2\mu^{(1)}\varphi_0}{r_1^2}\sum_{m=-\infty}^{\infty}\sum_{n=-\infty}^{\infty}\left(J_{m-n}\left(\alpha_1 d\right)\mathrm{i}E_{41}^{(3)}\left(\alpha_1 r_1\right)D_n+J_{m-n}\left(\beta_1 d\right)E_{42}^{(3)}\left(\beta_1 r_1\right)F_n\right)\mathrm{e}^{\mathrm{i}m\theta_1}. \tag{16b}$$

where $E_{ij}^{(k)}$, $M_{ij}^{(k)}$ are the contribution of various waves for stress and displacement, which are presented in the Appendix.

Finally, at the interfaces $r_1=a$ and $r_2=b$, the model assumes that tractions satisfy the Young-Laplace equations and displacements are continuous across the interface.

$$u_{r_1}^{(0)}=u_{r_1}^{(1)},\quad u_{\theta_1}^{(0)}=u_{\theta_1}^{(1)},\quad r_1=a \tag{17a}$$

$$u_{r_2}^{(1)}=u_{r_2}^{(2)},\quad u_{\theta_2}^{(1)}=u_{\theta_2}^{(2)},\quad r_2=b \tag{17b}$$

$$\begin{cases}\sigma_{r_1\theta_1}^{(0)}-\sigma_{r_1\theta_1}^{(1)}=-s_2(1-\nu^{(0)})\dfrac{\partial\sigma_{\theta_1\theta_1}^{(0)}}{\partial\theta_1}+s_2\nu^{(0)}\dfrac{\partial\sigma_{r_1r_1}^{(0)}}{\partial\theta_1}\\ \sigma_{r_1\theta_1}^{(0)}-\sigma_{r_1\theta_1}^{(1)}=-s_2(1-\nu^{(0)})\dfrac{\partial\sigma_{\theta_1\theta_1}^{(0)}}{\partial\theta_1}+s_2\nu^{(0)}\dfrac{\partial\sigma_{r_1r_1}^{(0)}}{\partial\theta_1}\end{cases},\quad r_1=a \tag{18}$$

$$\begin{cases}\sigma_{r_2r_2}^{(2)}-\sigma_{r_2r_2}^{(1)}=s_1(1-\nu^{(2)})\sigma_{\theta_2\theta_2}^{(2)}-s_1\nu^{(2)}\sigma_{r_2r_2}^{(2)}\\ \sigma_{r_2\theta_2}^{(2)}-\sigma_{r_2\theta_2}^{(1)}=-s_1(1-\nu^{(2)})\dfrac{\partial\sigma_{\theta_2\theta_2}^{(2)}}{\partial\theta_2}+s_1\nu^{(2)}\dfrac{\partial\sigma_{r_2r_2}^{(2)}}{\partial\theta_2}\end{cases},\quad r_2=b \tag{19}$$

Here

$$s_1=\frac{2\mu^s+\lambda^s}{2\mu^{(1)}b}=\eta s_2,\quad s_2=\frac{2\mu^s+\lambda^s}{2\mu^{(1)}a},\quad \eta=\frac{a}{b}. \tag{20}$$

By boundary condition Eqs. (17)-(19) on the surface, using the orthogonality of $\mathrm{e}^{in\theta}$, we obtained a set of equations with the unknown coefficients.

$$\sum_{n=-\infty}^{\infty}\left(J_{n-l}\left(\alpha_1 d\right)M_{71}^{(1)}\left(\alpha_1 b\right)C_n+J_{n-l}\left(\beta_1 d\right)\mathrm{i}M_{72}^{(1)}\left(\beta_1 b\right)E_n\right)$$

 Copyright © 2019 Isaac Scientific Publishing

$$+M_{71}^{(3)}\left(\alpha_1 b\right)D_l+\mathrm{i}M_{72}^{(3)}\left(\beta_1 b\right)F_l-M_{71}^{(1)}\left(\alpha_2 b\right)G_l-\mathrm{i}M_{72}^{(1)}\left(\beta_2 b\right)K_l=0\,, \tag{21}$$

$$\sum_{n=-\infty}^{\infty}\left(J_{n-l}\left(\alpha_1 d\right)\mathrm{i}M_{81}^{(1)}\left(\alpha_1 b\right)C_n+J_{n-l}\left(\beta_1 d\right)M_{82}^{(1)}\left(\beta_1 b\right)E_n\right)$$
$$+\mathrm{i}M_{81}^{(1)}\left(\alpha_1 b\right)D_l+M_{82}^{(3)}\left(\beta_1 b\right)F_l-\mathrm{i}M_{81}^{(1)}\left(\alpha_2 b\right)G_l-M_{82}^{(1)}\left(\beta_2 b\right)K_l=0\,, \tag{22}$$

$$\sum_{n=-\infty}^{\infty}\left(J_{l-n}\left(\alpha_1 d\right)M_{71}^{(3)}\left(\alpha_1 a\right)D_n+J_{l-n}\left(\beta_1 d\right)\mathrm{i}M_{72}^{(3)}\left(\beta_1 a\right)F_n\right)$$
$$-\mathrm{i}^{l}M_{71}^{(1)}\left(\alpha a\right)-M_{71}^{(3)}\left(\alpha a\right)A_l-\mathrm{i}M_{72}^{(3)}\left(\beta a\right)B_l+M_{71}^{(1)}\left(\alpha_1 a\right)C_l+\mathrm{i}M_{72}^{(1)}\left(\beta_1 a\right)E_l=0\,, \tag{23}$$

$$\sum_{n=-\infty}^{\infty}\left(J_{l-n}\left(\alpha_1 d\right)\mathrm{i}M_{81}^{(3)}\left(\alpha_1 a\right)D_n+J_{l-n}\left(\beta_1 d\right)M_{82}^{(3)}\left(\beta_1 a\right)F_n\right)$$
$$-\mathrm{i}^{l+1}M_{81}^{(1)}\left(\alpha a\right)-\mathrm{i}M_{81}^{(3)}\left(\alpha a\right)A_l-M_{82}^{(3)}\left(\beta a\right)B_l+\mathrm{i}M_{81}^{(1)}\left(\alpha_1 a\right)C_l+M_{82}^{(1)}\left(\beta_1 a\right)E_l=0\,, \tag{24}$$

$$\frac{\mu^{(1)}}{\mu^{(2)}}\sum_{n=-\infty}^{\infty}\left(J_{n-l}\left(\alpha_1 d\right)E_{11}^{(1)}\left(\alpha_1 b\right)C_n+J_{n-l}\left(\beta_1 d\right)\mathrm{i}E_{12}^{(1)}\left(\beta_1 b\right)E_n\right)$$
$$-E_{11}^{(1)}\left(\alpha_2 b\right)G_l-\mathrm{i}E_{12}^{(1)}\left(\beta_2 b\right)K_l+\frac{\mu^{(1)}}{\mu^{(2)}}\left(E_{11}^{(3)}\left(\alpha_1 b\right)D_l+\mathrm{i}E_{12}^{(3)}\left(\beta_1 b\right)F_l\right)$$
$$-s_1\nu\left(E_{11}^{(1)}\left(\alpha_2 b\right)G_l+\mathrm{i}E_{12}^{(1)}\left(\beta_2 b\right)K_l\right)$$
$$+s_1\left(1-\nu\right)\left(E_{21}^{(1)}\left(\alpha_2 b\right)G_l+\mathrm{i}E_{22}^{(1)}\left(\beta_2 b\right)K_l\right)=0\,, \tag{25}$$

$$\frac{\mu^{(1)}}{\mu^{(2)}}\sum_{n=-\infty}^{\infty}\left(J_{n-l}\left(\alpha_1 d\right)\mathrm{i}E_{41}^{(1)}\left(\alpha_1 b\right)C_n+J_{n-l}\left(\beta_1 d\right)E_{42}^{(1)}\left(\beta_1 b\right)E_n\right)$$
$$+\frac{\mu^{(1)}}{\mu^{(2)}}\left(\mathrm{i}E_{41}^{(3)}\left(\alpha_1 b\right)D_l+E_{42}^{(3)}\left(\beta_1 b\right)F_l\right)-\mathrm{i}E_{41}^{(1)}\left(\alpha_2 b\right)G_l-E_{42}^{(1)}\left(\beta_2 b\right)K_l$$
$$+s_1\nu\left(E_{11}^{(1)}\left(\alpha_2 b\right)G_l+\mathrm{i}E_{22}^{(1)}\left(\beta_2 b\right)K_l\right)\mathrm{i}l$$
$$-s_1\left(1-\nu\right)\left(E_{21}^{(1)}\left(\alpha_2 b\right)G_l+\mathrm{i}E_{22}^{(1)}\left(\beta_2 b\right)K_l\right)\mathrm{i}l=0\,, \tag{26}$$

$$\frac{\mu^{(1)}}{\mu^{(0)}}\sum_{n=-\infty}^{\infty}\left(J_{l-n}\left(\alpha_1 d\right)E_{11}^{(3)}\left(\alpha_1 a\right)D_n+\mathrm{i}J_{l-n}\left(\beta_1 d\right)E_{12}^{(3)}\left(\beta_1 a\right)F_n\right)$$
$$+\frac{\mu^{(1)}}{\mu^{(0)}}\left(E_{11}^{(1)}\left(\alpha_1 a\right)C_l+\mathrm{i}E_{12}^{(1)}\left(\beta_1 a\right)E_l\right)-E_{11}^{(1)}\left(\alpha a\right)\mathrm{i}^{l}-E_{11}^{(3)}\left(\alpha a\right)A_l-\mathrm{i}E_{12}^{(3)}\left(\beta a\right)B_l$$
$$+s_2\left(1-\nu\right)\left(E_{21}^{(1)}\left(\alpha a\right)\mathrm{i}^{l}+E_{21}^{(3)}\left(\alpha a\right)A_l+\mathrm{i}E_{22}^{(3)}\left(\beta a\right)B_l\right)$$
$$-s_2\nu\left(E_{11}^{(1)}\left(\alpha a\right)\mathrm{i}^{l}+E_{11}^{(3)}\left(\alpha a\right)A_l+\mathrm{i}E_{12}^{(3)}\left(\beta a\right)B_l\right)=0\,, \tag{27}$$

$$\frac{\mu^{(1)}}{\mu^{(0)}}\sum_{n=-\infty}^{\infty}\left(J_{l-n}\left(\alpha_1 d\right)\mathrm{i}E_{41}^{(3)}\left(\alpha_1 a\right)D_n+J_{l-n}\left(\beta_1 d\right)E_{42}^{(3)}\left(\beta_1 a\right)F_n\right)$$
$$+\frac{\mu^{(1)}}{\mu^{(0)}}\left(\mathrm{i}E_{41}^{(1)}\left(\alpha_1 a\right)C_l+E_{42}^{(1)}\left(\beta_1 a\right)E_l\right)-E_{41}^{(1)}\left(\alpha a\right)\mathrm{i}^{l+1}-iE_{41}^{(3)}\left(\alpha a\right)A_l-E_{42}^{(3)}\left(\beta a\right)B_l$$
$$+s_2\nu\left(E_{11}^{(1)}\left(\alpha a\right)\mathrm{i}^{l}+E_{11}^{(3)}\left(\alpha a\right)A_l+\mathrm{i}E_{12}^{(3)}\left(\beta a\right)B_l\right)\mathrm{i}l$$
$$-s_2\left(1-\nu\right)\left(E_{21}^{(1)}\left(\alpha a\right)\mathrm{i}^{l}+E_{21}^{(3)}\left(\alpha a\right)A_l+\mathrm{i}E_{22}^{(3)}\left(\beta a\right)B_l\right)\mathrm{i}l=0\,, \tag{28}$$

Copyright © 2019 Isaac Scientific Publishing

3 Results and Discussion

We define the dynamic stress concentration factor (DSCF) as

$$\mathrm{DSCF} = \left| \frac{\sigma_{\theta\theta}^{(0)}}{\sigma_0} \right| \tag{29}$$

where $\sigma_{\theta\theta}^{(0)}$ is the bulk stress of the matrix material at interface $r_1=a$, $\sigma_0 = \mu^{(0)}\beta_0^2\phi_0$ is the stress intensity in the propagation direction of P-wave.

To confirm our numerical results, comparisons with the published results for special cases under low frequency incident waves are shown in Fig. 2. When the material properties of the coating and the core are identical and d=0(e=0) the results for the P wave-induced DSCF are in good agreement with those presented in [24].

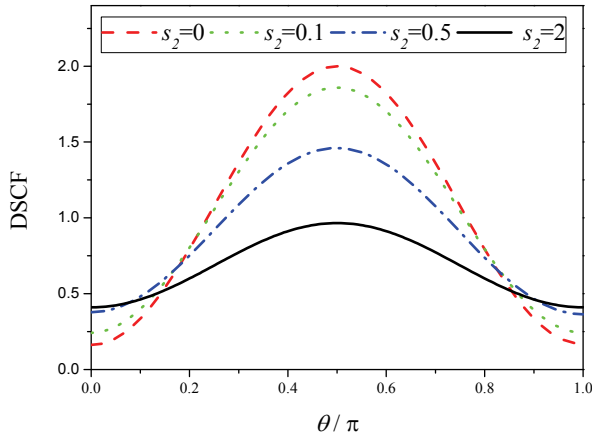

Figure 2. Comparisons of our numerical results with the results of Ou *et al.* [24] at interface (r_1=a) with various values of S_2 for the DSCF with $\alpha_0 a$=0.1, η=1.1, $\mu^{(1)}/\mu^{(0)}$=0.2 and α_1/α_0=3.

To make the follow calculations tractable, we assume that the properties of the inclusion and matrix were identical, but different from those of coating. Let η=a/b=2, ec=d/a–b.

3.1 The Effects of a Low Frequency Incident Wave with $\alpha_0 a = 0.1$

In this case, the wavelength λ=20πa of the incident wave is much larger than the radius of the coating and core. The distributions of DSCF near the surface (r_1=a) for different values of S_2 and $\mu^{(1)}/\mu^{(0)}$ are shown in Fig. 3 and 4. It can be seen from Fig. 3 that results are significant for the effect of the interface stress on the dynamic stress concentration. When S_2 increased, the DSCF decreased considerably around θ=±π/2, while it slightly increased around θ=0 and θ=±π. In Fig. 4, when the $\mu^{(1)}/\mu^{(0)}$ increased, the DSCF decreased significantly around θ=±π/2, and slightly increased around θ=0 and θ=±π. For softer inclusion ($\mu^{(1)}/\mu^{(0)}$<1), the maximum DSCF appeared at θ=±π/2. For hard inclusion ($\mu^{(1)}/\mu^{(0)}$>1), the maximum DSCF appeared at θ=0 and θ=±π.

 Copyright © 2019 Isaac Scientific Publishing

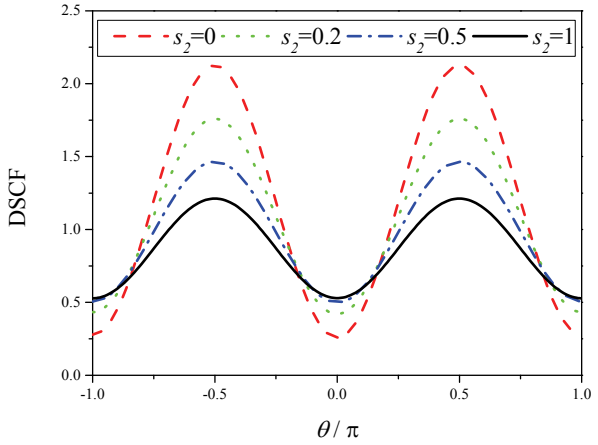

Figure 3. Distribution of DSCF along interface (r_1=a) with various values of S_2 under $\alpha_0 a$=0.1, η=2, e=0.5, $\mu^{(1)}/\mu^{(0)}$=0.1, α_1/α_0=3.

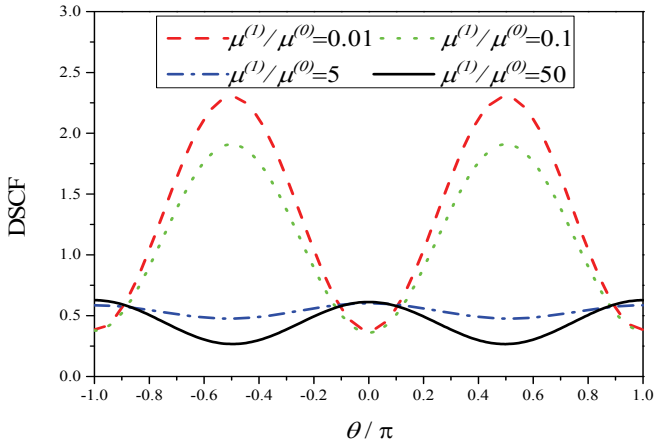

Figure 4. Distribution of DSCF along interface (r_1=a) with various values of $\mu^{(1)}/\mu^{(0)}$ under $\alpha_0 a$=0.1, S_2=0.1, η=2, e=0.5.

3.2 The Effects of a High Frequency Incident Wave $\alpha_0 a = \pi$

In this case, the wavelength equals the diameter of the coated inclusion, Fig. 5 and 6 show the distribution of DSCF along interface (r_1=a) near the coated inclusion, and the magnitude of the DSCF was generally lower than that of a low frequency incident wave. Multiple peak values are excited along the interface due to the interference between the incident and reflected waves. Fig. 5 shows that the maximum value of DSCF continuously decreases with increasing S_2. For different ratio of shear moduli ($\mu^{(1)}/\mu^{(0)}$), the variation of the DSCF is show in Fig. 6. For softer inclusion ($\mu^{(1)}/\mu^{(0)}$<1), the ratio of shear moduli had little influence on the DSCF; For hard inclusion ($\mu^{(1)}/\mu^{(0)}$>1), the maximum value of DSCF was smaller than that of a hard inclusion, Different from the case of a low frequency incident wave. Fig. 7 shows that DSCF increased with the increased of eccentricity at θ=±π/2. Fig. 8 shows that the distribution of image is more complex than low frequency.

Copyright © 2019 Isaac Scientific Publishing

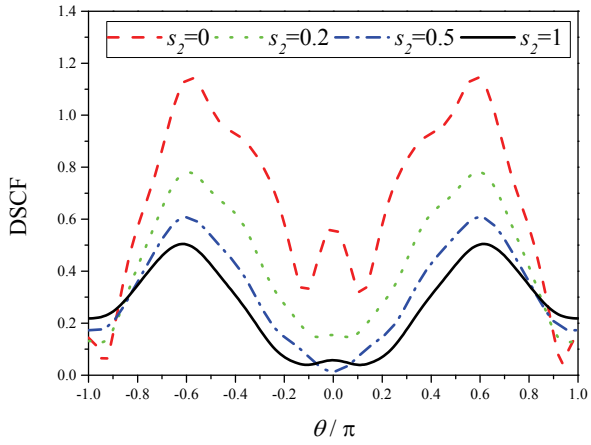

Figure 5. Distribution of DSCF along interface (r_1=a) with various values of S_2 under $\alpha_0 a$=π, η=2, e=0.5, $\mu^{(1)}/\mu^{(0)}$=0.1, α_1/α_0=0.3.

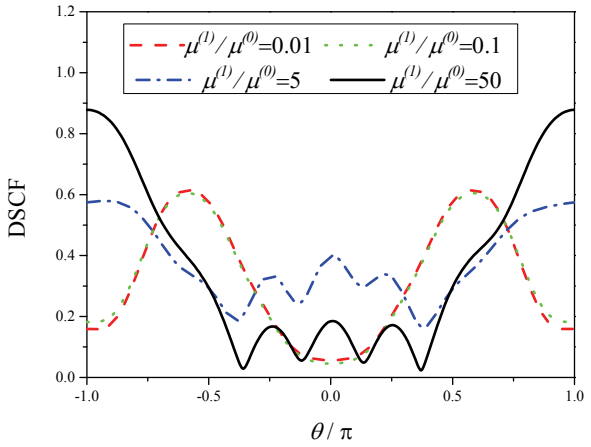

Figure 6. Distribution of DSCF along interface (r_1=a) with various values of $\mu^{(1)}/\mu^{(0)}$ under $\alpha_0 a$=0.1, S_2=0.5, η=2, e=0.5, α_1/α_0=0.3.

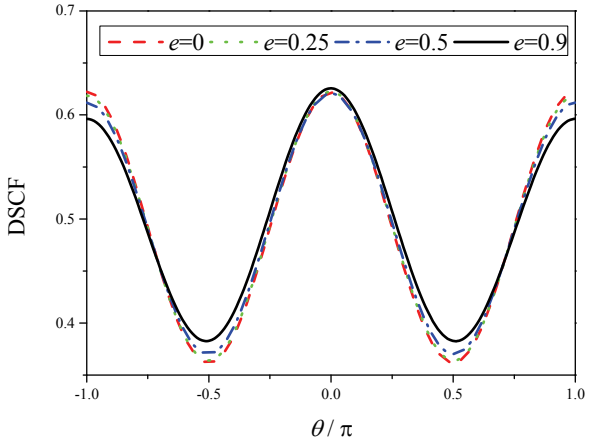

Figure 7. Distribution of DSCF along interface (r_1=a) with various values of eccentricity under $\alpha_0 a$=0.1, η=2, S_2=0.5, $\mu^{(1)}/\mu^{(0)}$=10, α_1/α_0=0.3.

Copyright © 2019 Isaac Scientific Publishing

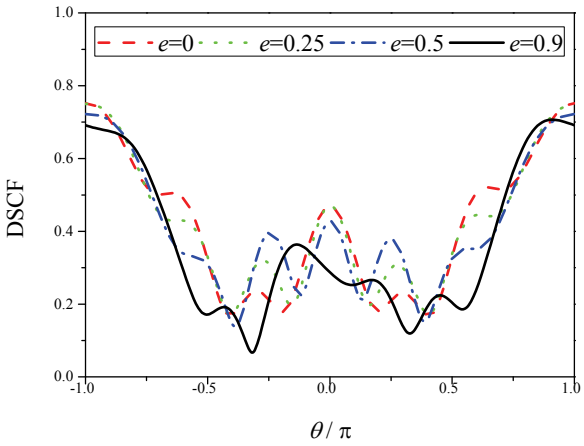

Figure 8. Distribution of DSCF along interface (r_1=a) with various values of eccentricity under $\alpha_0 a$=π, η=2, S_2=0.5, $\mu^{(1)}/\mu^{(0)}$=10, α_1/α_0=0.3.

4 Conclusion

Using the addition theorem and wave functions expansion method, the scattering of plane compressional waves by a cylinder with an eccentric inclusion are investigated. The effects of wave number, surface effects, softer/hard inclusion and eccentricity on dynamic stress concentration as the radius of the inclusion reduce to the nanoscale are analyzed. We conclude that the interface effects become significant and are taken into account as the radius of the inclusion is decreased to the nanoscale.

Acknowledgments. The supports from the National Natural Science Foundation (Grant No. 11362009 and No. 11862014) are acknowledged.

References

1. Hasheminejad S.M., Kazemirad, S. (2008) Dynamic vicoelastic effects on sound wave scattering by an eccentriccompound circular cylinder. Journal of Sound and Vibration, 318, 506-526.
2. Hasheminejad S.M., Kazemirad, S. (2008) Dynamic response of an eccentrically lined circular tunnel in poroelastic soil under seismic excitation. Soil Dynamics and Earthquake Engineering, 28, 277–292.
3. Hasheminejad S.M., Kazemirad, S. (2008) Scattering and absorption of sound by a compound cylindrical porous absorber with an eccentric core. A Cta a Custica United with a Custica, 94, 79-90.
4. Mushref, M.A. (2005) TM radiation from an eccentric dielectric coated cylinder with two Infinite Slots. Journal of Electromagnetic Waves and Applications, 19, 577-590.
5. Simao, A.G., Guimaraes, L.G. (1999) Electromagnetic stress on resonant light scattering by a cylinder with an eccentric inclusion. Optics Communications, 170, 137–148.
6. Roumeliotis, J.A., Fikioris, J.G. (1980) Cutoff wauenumbers and the field of surface wave modes of an eccentric circular goubau waveguide. Journal of the Frankiin Institmte Pergmon Press Ltd, 309, 309-325.
7. Pattanayak, R.K., Krishnan, P.M. (2015) Low frequency axisymmetric longitudinal guided waves in eccentric annular cylinders. Journal of the Acoustical Society of America, 137, 3253-3262.
8. Mushref, M.A. (2007) Matrix solution to electromagnetic scattering by a conducting cylinder with an eccentric metamaterial coating. Journal of Mathematical Analysis and Applications, 332, 356–366.
9. Yousif, H.A., Elsherbeni, A.Z. (1999) Electromagnetic scattering from an eccentric multilayered cylinder at oblique incidence. Journal of Electromagnetic Waves and Applications, 13, 325-336.
10. Weber, W., Zastrau, B.W. (2011) Non-plane wave scattering from a single eccentric circular incusion- Part 1:SH waves. Journal of the Oretical and Applied Mechanics, 49, 1183-1201.
11. Huang, W., Wang, Y.J. and Rokhlin, S.I. (1996)Oblique scattering of an elastic wave from a multilayered cylinder in a solid. Journal of Acoustical Society of America, 99, 2742-2754.
12. Qin, B., Chen, J.J. and Cheng, J.C. (2005) Local resonant characteristics of a layerde cylinder embedded in the

Copyright © 2019 Isaac Scientific Publishing

elastic mediun. Chinese Physics, 14, 2522-2528.
13. Hasheminejad, S. M., Rajabi, M. (2007) Acoustic resonance scattering from a submerged functionally graded cylindrical shell. Journal of Sound and Vibration, 302, 208-228.
14. Shindo, Y., Niwa, N. (1996) Scattering of antiplane shear waves in a fiber-reinforced composite medium with interfacial layers.Acta Mechanica, 117, 181-190.
15. Li, F.M., Hu, C. and Huang, W.H. (2002)Scattering of elastic waves in an elastic matrix containing an inclusion with interfaces. Acta Mechanica Solida Sinica, 15, 270-276.
16. Nersisyan, H.B., Matevosyan, H.H. (2011) Scattering and transformation of waves on heavy particles in magnetized plasma. Journal of Modern Physics, 2, 162-173.
17. Godoy, S., Villa, K. (2016) A basis for causal scattering waves, relativistic diffraction in time functions. Journal of Modern Physics, 7, 1181-1191.
18. Yahya, G.A., Elhag, S.H. and Sanaa, M.F. (2014) Effect of initial stress on wave frequencies of elastic solid with rotation. Journal of Modern Physics, 5, 2012-2021.
19. Volobuev, A.N., Petrov, E.S. (2011) Angular distribution of photoelectrons during irradiation of metal surface by electromagnetic waves. Journal of Modern Physics, 2, 780-786.
20. El-Shorbagy, K.H., Al-Fhaid, A.S. and Al-Ghamdi, M.A. (2011) Separation method in the problem of a beam-plasma interaction in a cylindrical warm plasma waveguide. Journal of Modern Physics, 2, 1104-1108.
21. Wang, G.F., Wang, T.J. (2006) Surface effects on the diffraction of plane compressional waves by a nanosized circular hole. Applied Physics Letters, 89, 1-3.
22. Wang, G.F. (2006) Multiple diffraction of plane compressional waves by two circular cylindrical holes with surface effects. Journal of Applied Physics, 105, 1-6.
23. Ru, Y., Wang, G.F. and Wang, T.J. (2009) Diffractions of elastic waves and stress concentration near a cylindrical nano-Inclusion incorporating surface effect. Vibration and Acoustics, 131, 1-7.
24. Ou, Z.Y., Lee, D.W. (2012) Effects of interface energy on scattering of plane elastic wave by a nano-sized coated fiber. Journal of Sound and Vibration, 331, 5623-5643.
25. Ou, Z.Y., Lee, D.W. (2012) Effects of interface energy on multiple scattering of plane compressional waves by two cylindrical fibers. International Journal of Applied Mechanics, 4, 1-19.

Appendix

$$M_{71}^{(1)}\left(\alpha r\right)=-nJ_n\left(\alpha r\right)+\alpha rJ_{n-1}\left(\alpha r\right)$$

$$M_{71}^{(3)}\left(\alpha r\right)=-nH_n^{(1)}\left(\alpha r\right)+\alpha rH_{n-1}^{(1)}\left(\alpha r\right)$$

$$M_{72}^{(1)}\left(\beta r\right)=nJ_n\left(\beta r\right)$$

$$M_{72}^{(3)}\left(\beta r\right)=nH_n^{(1)}\left(\beta r\right)$$

$$M_{81}^{(1)}\left(\alpha r\right)=nJ_n\left(\alpha r\right)$$

$$M_{81}^{(3)}\left(\alpha r\right)=nH_n^{(1)}\left(\alpha r\right)$$

$$M_{82}^{(1)}\left(\beta r\right)=nJ_n\left(\beta r\right)-\beta rJ_{n-1}\left(\beta r\right)$$

$$M_{82}^{(3)}\left(\beta r\right)=nH_n^{(1)}\left(\beta r\right)-\beta rH_{n-1}^{(1)}\left(\beta r\right)$$

$$E_{11}^{(1)}\left(\alpha r\right)=\left(n^2+n-1/2\,\beta^2r^2\right)J_n\left(\alpha r\right)-\alpha rJ_{n-1}\left(\alpha r\right)$$

$$E_{11}^{(3)}\left(\alpha r\right)=\left(n^2+n-1/2\,\beta^2r^2\right)H_n^{(1)}\left(\alpha r\right)-\alpha rH_{n-1}^{(1)}\left(\alpha r\right)$$

$$E_{12}^{(1)}\left(\beta r\right)=-\left(n^2+n\right)J_n\left(\beta r\right)+n\beta rJ_{n-1}\left(\beta r\right)$$

$$E_{12}^{(3)}\left(\beta r\right)=-\left(n^2+n\right)H_n^{(1)}\left(\beta r\right)+n\beta rH_{n-1}^{(1)}\left(\beta r\right)$$

$$E_{21}^{(1)}\left(\alpha r\right)=-\left(n^2+n+1/2\,\beta^2r^2-\alpha^2r^2\right)J_n\left(\alpha r\right)+\alpha rJ_{n-1}\left(\alpha r\right)$$

 Copyright © 2019 Isaac Scientific Publishing

$$E_{21}^{(3)}\left(\alpha r\right)=-\left(n^{2}+n+1/2\,\beta^{2}r^{2}-\alpha^{2}r^{2}\right)H_{n}^{(1)}\left(\alpha r\right)+\alpha rH_{n}^{(1)}\left(\alpha r\right)$$

$$E_{22}^{(3)}\left(\beta r\right)=\left(n^{2}+n\right)H_{n}^{(1)}\left(\beta r\right)-n\beta rH_{n-1}^{(1)}\left(\beta r\right)$$

$$E_{41}^{(1)}\left(\alpha r\right)=-\left(n^{2}+n\right)J_{n}\left(\alpha r\right)+n\alpha rJ_{n-1}\left(\alpha r\right)$$

$$E_{41}^{(3)}\left(\alpha r\right)=-\left(n^{2}+n\right)H_{n}^{(1)}\left(\alpha r\right)+n\alpha rH_{n-1}^{(1)}\left(\alpha r\right)$$

$$E_{42}^{(1)}\left(\beta r\right)=-\left(n^{2}+n-1/2\,\beta^{2}r^{2}\right)J_{n}\left(\beta r\right)+\beta rJ_{n-1}\left(\beta r\right)$$

$$E_{42}^{(3)}\left(\beta r\right)=-\left(n^{2}+n-1/2\,\beta^{2}r^{2}\right)H_{n}^{(1)}\left(\beta r\right)+\beta rH_{n-1}^{(1)}\left(\beta r\right)$$

Copyright © 2019 Isaac Scientific Publishing